



**HAL**  
open science

## Quantitative Pollutant Modelling: an Essential Prerequisite for Diesel HCCI and LTC Engine Design

V. Knop, H. Kircher, S. Jay, Ph. Béard, A. Pires da Cruz, O. Colin

► **To cite this version:**

V. Knop, H. Kircher, S. Jay, Ph. Béard, A. Pires da Cruz, et al.. Quantitative Pollutant Modelling: an Essential Prerequisite for Diesel HCCI and LTC Engine Design. Oil & Gas Science and Technology - Revue d'IFP Energies nouvelles, 2008, 63 (4), pp.495-515. 10.2516/ogst:2008022 . hal-02002030

**HAL Id: hal-02002030**

**<https://ifp.hal.science/hal-02002030>**

Submitted on 31 Jan 2019

**HAL** is a multi-disciplinary open access archive for the deposit and dissemination of scientific research documents, whether they are published or not. The documents may come from teaching and research institutions in France or abroad, or from public or private research centers.

L'archive ouverte pluridisciplinaire **HAL**, est destinée au dépôt et à la diffusion de documents scientifiques de niveau recherche, publiés ou non, émanant des établissements d'enseignement et de recherche français ou étrangers, des laboratoires publics ou privés.

# Quantitative Pollutant Modelling: an Essential Prerequisite for Diesel HCCI and LTC Engine Design

V. Knop, H. Kircher, S. Jay, Ph. Béard, A. Pires da Cruz and O. Colin

Institut français du pétrole, IFP, 1-4 avenue de Bois-Préau, 92852 Rueil-Malmaison Cedex - France

e-mail: vincent.knop@ifp.fr - henri.kircher@ifp.fr - stephane.jay@ifp.fr - philippe.beard@ifp.fr - antonio.pires-da-cruz@ifp.fr - olivier.colin@ifp.fr

## Résumé — Modélisation quantitativement prédictive des polluants : un pré-requis essentiel pour l'aide au développement des concepts HCCI et LTC Diesel

— Pour répondre aux exigences actuelles en termes d'efficacité et d'impact sur l'environnement des moteurs automobiles Diesel, les concepts de combustion HCCI (Homogeneous Charge Compression Ignition) et LTC (Low Temperature Combustion) ont été développés avec comme objectif la réduction des émissions polluantes à charge partielle tout en conservant les niveaux de consommation actuels. Afin d'être utile à l'optimisation de ces nouveaux modes de combustion, les logiciels de Mécanique des Fluides Numérique 3D ne doivent pas se limiter à prédire qualitativement la consommation et les émissions polluantes mais doivent s'orienter vers une prédiction quantitative de ces grandeurs. L'implantation de modèles prédictifs de combustion et de formation de polluants dans les codes de Mécanique des Fluides Numérique 3D est, par conséquent, un pré-requis pour l'utilisation des outils de conception assistée par ordinateur dans le cadre du développement de nouvelles géométries de chambre de combustion ou de nouvelles stratégies de fonctionnement.

La modélisation des émissions polluantes est une tâche très difficile car les phénomènes conduisant à l'apparition et à la conversion des espèces polluantes sont régis par des réactions de chimie complexe et ont lieu pendant ou juste après la formation du mélange et la combustion et dépendent donc en grande partie de ces deux phénomènes. Pour ajouter à la difficulté, ces réactions de chimie complexe ne sont actuellement pas complètement connues. La prédiction des émissions polluantes dans un outil d'analyse industriel nécessite, simultanément, une bonne prédiction de la formation du mélange et de la combustion ainsi qu'une réduction des schémas de cinétique chimique pour disposer de modèles prédictifs sans pour autant conduire à des temps de calcul prohibitifs.

Les concepts de combustion HCCI et LTC ont des plages de fonctionnement qui sont principalement limitées par le niveau de bruit issu de la combustion et le compromis entre émissions de  $\text{NO}_x$  et de suies. Le niveau de bruit est lié au déroulement de la combustion, et principalement au gradient de pression, ce qui fait dépendre la qualité de sa description de la qualité de la modélisation de la combustion. Le compromis entre émissions de suies et de  $\text{NO}_x$  ne peut lui être prédit que si des modèles fiables existent pour ces espèces. Dans la présente étude, le modèle de Zeldovitch étendu est utilisé pour les oxydes d'azote alors que le modèle PSK (*Phenomenological Soot Kinetics*), couplé au modèle CORK (*CO Reduced Kinetics*) pour assurer le bilan énergétique, vise à modéliser les émissions de suies.

**Abstract — Quantitative Pollutant Modelling: an Essential Prerequisite for Diesel HCCI and LTC Engine Design** — To face the demand for efficient and environmentally-friendly engines, the Diesel HCCI (Homogeneous Charge Compression Ignition) and LTC (Low Temperature Combustion) concepts have been developed in order to drastically reduce the pollutant emissions of present Diesel engines at

part load while maintaining their fuel consumption attractive. To be useful in the optimisation procedure of such new engine concepts, 3D CFD (Computational Fluid Dynamics) simulation softwares have to be predictive in terms of consumption and pollutants not only qualitatively (emphasising the global trends) but also quantitatively (providing reliable numbers to allow design or strategy comparisons). The implementation of accurate predictive combustion and pollutant models in 3D CFD codes are consequently a prerequisite to the use of these simulation tools to develop new combustion chamber designs or to test unconventional operating strategies.

Pollutant modelling is a very difficult task because the pollutant formation and conversion during and after combustion heavily depend on the mixture formation and combustion processes that define the initial conditions for their complex chemical reactions. Furthermore, the occurring complex chemical reactions are far from being totally known. The correct prediction of the mixture formation and combustion processes are therefore essential for a correct pollutant prediction. However, the complex chemistry controlling the pollutant formation needs to be reduced to propose models that give accurate results with a reasonable CPU time consumption.

For the HCCI and LTC engine concepts, the operating restrictions are mainly the  $\text{NO}_x$ /soot trade-off and the noise level. The noise level may be related to the pressure rise and its prediction will therefore be a matter of accurate combustion description. On the other hand, the  $\text{NO}_x$ /soot trade-off can only be numerically handled if accurate pollutant models are available. In the present study, the  $\text{NO}_x$  model is the extended Zeldovich model while the soot model is the PSK (Phenomenological Soot Kinetics) model coupled with the CORK (CO Reduced Kinetics) model to ensure a correct energy balance.

## ACRONYMS

CFD	Computational Fluid Dynamics
CORK	CO Reduced Kinetics
CRI	Common Rail Injection
ECFM3Z	3-Zone Extended Coherent Flame Model
EGR	Exhaust Gas Recirculation
EUDC	Extra-Urban Driving Cycle
EVO	Exhaust Valve Opening
FAER	Fuel/Air Equivalence Ratio
HCCI	Homogeneous Charge Compression Ignition
IMEP	Indicated Mean Effective Pressure
ISFC	Indicated Specific Fuel Consumption
LTC	Low Temperature Combustion
NADI	Narrow Angle Direct Injection
NEDC	New European Driving Cycle
PAH	Polycyclic Aromatic Hydrocarbons
PDF	Probability Density Function
PSK	Phenomenological Soot Kinetics
TDC	Top Dead Center
TKI	Tabulated Kinetics of Ignition

## INTRODUCTION

Today, the demand for cleaner and more fuel-efficient engines is driving the research and development field. These demands may appear as contradictory when optimising the

traditional combustion concepts and lead to the creation of alternative concepts. Among these concepts, the Diesel HCCI and LTC combustion modes aim to reduce the exhaust emissions through a low temperature combustion while retaining most of the fuel consumption benefits related to the conventional Diesel engines at part load. Nevertheless, even for such promising combustion concepts, a trade-off between the different types of exhaust emissions and the fuel economy still exists. In such a context, 3D Computational Fluid Dynamics (CFD) has long been used to better understand the origin of some experimentally observed trends and/or to optimise the engine layouts to fully benefit from these new combustion concepts. The ever stricter legal demands for lower pollutant emissions induce a progressive shift in the required capabilities of the 3D CFD codes. Providing accurate trends and qualitatively explaining the consequences of some design choices are not enough anymore. The present demands are a quantitative prediction of the pollutant emissions to be able to balance the potential gains in engine-out emissions with the possible fuel penalty or with totally different engine designs, for example, a less complex and cheaper combustion setup coupled with a more refined combination of after-treatment devices.

In the field of Diesel engines, the introduction of the HCCI and LTC combustion modes allows a wide reduction of the engine-out  $\text{NO}_x$  emissions thanks to a low temperature combustion [1]. On the other hand, the reduction of the mean in-cylinder temperature impedes the oxidation

during the expansion stroke of the soot particles produced during the diffusion part of the combustion. The use of cooled recirculated burnt gases to maintain a low temperature during combustion worsens this phenomenon because it also reduces the amount of oxygen molecules available to oxidise the soot particles and the probability of interaction between oxygen and soot. Consequently, even if the HCCI and LTC concepts produce far lower engine-out  $\text{NO}_x$  emissions than the conventional Diesel combustion mode [1], the trade-off between  $\text{NO}_x$  and soot emissions is still a key point for future Diesel engines. To fully benefit from the low temperature combustion potential, the engine design must therefore focus on the reduction of the engine-out soot emissions by proposing combustion chamber layouts and injection strategies that reduce the soot formation or enhance the soot oxidation. The Narrow Angle Direct Injection™ (NADI™) concept developed at IFP is thought to be able to meet these demands because of its ability to directly act on the local degree of mixture heterogeneity.

To be able to optimise such a concept, the 3D CFD tools are of prime importance to understand the existing designs and to propose improvements. Nevertheless, this optimisation task may only be efficiently performed if quantitative pollutant models are available which is today a major development axis for all 3D CFD codes. The difficulty of quantitative engine-out pollutant modelling has multiple sources:

- The lack of complete knowledge about the pollutant formation paths due to the extreme complexity of the chemistry, in particular, when studying real fuels containing hundreds of hydrocarbon species;
- The dependency of these paths on the in-cylinder conditions induced by various physical phenomena occurring in the cylinder before any pollutant formation (*i.e.* injection, mixture formation, auto-ignition, combustion spreading) whose modelling quality has a fundamental impact on the predictivity of the computed pollutant levels;
- The necessity to produce predictive results in a reasonable time frame to be actually integrated in the design process. By today standards, the simulation of the closed-valves part of the engine cycle must be performed in about 4 hours with an up-to-date supercomputer and a meshing with 1 mm typical length scale.

Summing these difficulties explains the challenge of pollutant modelling and the necessity to evaluate the 3D CFD simulation results as a whole. Indeed, there is no sense in judging the predicted engine-out pollutant emissions if the combustion process or the in-cylinder pressure evolution are not accurately reproduced. In such a case, the in-cylinder physical conditions are obviously not correctly simulated and, whatever the quality of the pollutant modelling results, they cannot be considered as coming from a predictive modelling.

When known or partially known, the set of chemistry reactions representing the pollutant formation and conversion processes often contains a large number of species and reactions. Some authors have made the choice to directly couple these detailed kinetics chemistry schemes with the flow solver [2-4]. The advantage of this approach is to guarantee a control of the simulation accuracy by the complexity of the chosen chemistry but the consequence is unaffordable CPU times for everyday engineering applications. An alternative approach is to focus on reduced schemes derived from detailed chemistry or on phenomenological schemes to benefit from most of the complex chemistry accuracy while maintaining a low CPU time consumption [5-11]. Finally, independent modelling of each regulated pollutant is neither realistic nor efficient. For example, as identified in detailed kinetics studies, the soot and CO kinetics are strongly coupled due to the presence of common species in both schemes.

In the present work, the phenomenological approach is used to model three of the main regulated pollutants: nitrogen oxides, carbon monoxide and soot particles. The  $\text{NO}_x$  emissions are modelled with the extended Zeldovitch model. The CO formation model, called CO Reduced Kinetics (CORK), is an original 6-step mechanism developed at IFP [12]. The soot particle model, called Phenomenological Soot Kinetics (PSK), is an 8-step mechanism also developed at IFP [7]. To account for the chemical interaction between the CO and soot formation paths, these two models are coupled through the consideration of common species and chemical reactions linking some of them [12]. Furthermore, they are also fully coupled with the ECFM3Z combustion model in terms of species and energy balances.

With near-zero  $\text{NO}_x$  emissions at low load, the NADI™ concept is particularly efficient in terms of emission reduction in the urban part of the NEDC legal driving cycle. Therefore, the challenge is to optimise the engine design and the operating strategies to also reach benefits for the highest loads in the EUDC part of the cycle. With today's designs and strategies, the corresponding operating points are located near the high load limit of the LTC operating region of the engine on either side of this limit. These points are characterised by a high "sooting" tendency that prevents from fully benefiting of the EGR strategy to reduce the engine-out  $\text{NO}_x$  emissions. In such a case, the quantitative prediction of the soot and  $\text{NO}_x$  emissions is a crucial element to be able to optimise the chamber design. Furthermore, the use of simplified pollutant models with fitted constants valid for a restricted speed – load range is not conceivable because the piston design optimisation cannot only be performed for these particular operating points. Any design improving the emissions on these operating points must also be tested for full load and low load operating points in order to avoid an emission increase in

the urban part of the cycle or a reduction of the peak engine power output, which would be “commercially” unacceptable.

## 1 THE 3D CFD CODE

IFP-C3D is a 3D CFD parallel code developed at IFP solving the Navier-Stokes equations using an extended Arbitrary Lagrangian Eulerian finite volume method on unstructured and conformal hexahedral meshes [13]. In the present study, an internal grid generator creates wedge-type meshes and turbulence is modelled with the  $k$ - $\epsilon$  RNG model. Combustion modelling is the combination of a sub-grid mixture descriptor, the 3-Zone Extended Coherent Flame Model (ECFM3Z) [14, 15], a chemical kinetics descriptor, the TKI auto-ignition model [16, 17] and a high temperature fuel oxidation mechanism, the CORK model. To obtain a realistic spray modelling during the injector needle motion, the Transient Injection Conditions model [18] is used.

## 2 COMBUSTION MODELLING

For compression ignition internal combustion engines, the combustion process is generally described as a blend of two elementary combustion modes: premixed combustion and diffusion flame. Purely premixed combustion is obtained for a perfectly homogeneous mixture with appropriate conditions. In other words, it is a combustion mode appearing when the mixture formation process already came to an end. Pure diffusion flame is a mixture-controlled combustion mode. The predominant influence of mixture is due to the longer time scales of the mixture process with respect to the fuel oxidation process. Therefore, mixture and combustion are sequentially combined for premixed combustion and

simultaneously combined for diffusion flame but both processes are of equal importance whatever the combustion mode.

Real-life combustion in Diesel engines is a more complex combination of mixture and fuel oxidation processes than the exemplifications that are the chemically-controlled premixed combustion and the mixing-controlled diffusion flame. Nevertheless, the basics of such academic combustion modes are still present. For conventional Diesel combustion, the early-injected fuel has time to efficiently mix with air before auto-ignition locally occurs and mainly burns in a premixed mode, while the late-injected fuel is consumed in a diffusion flame mode as soon as droplets evaporate. Consequently, Diesel combustion modelling requires dedicated models to represent the mixing process and the fuel oxidation in various conditions. Furthermore, to accurately model the behaviour of any Diesel-fuelled engine, the models must be able to dynamically interact depending on the local in-cell conditions.

In the present work, the turbulent mixing process is described with the ECFM3Z model [14, 15]. Once combustion starts, this model defines a fresh gas zone and a burnt gas zone. The combustion in the fresh gas zone is described with the TKI model [16, 17] which accounts for chemical kinetics. The fuel oxidation in the burnt gas zone is described with the CORK model. The combustion in the fresh gases can basically be seen as the premixed part of combustion while that in the burnt gases is due to the late addition of fuel in the cell by the spray evaporation and relates to diffusion flame. The ECFM3Z and TKI models are described hereafter. The CORK model description is located in the pollutant modelling section as it is also responsible for the prediction of carbon monoxide emissions and directly coupled with the soot prediction model.

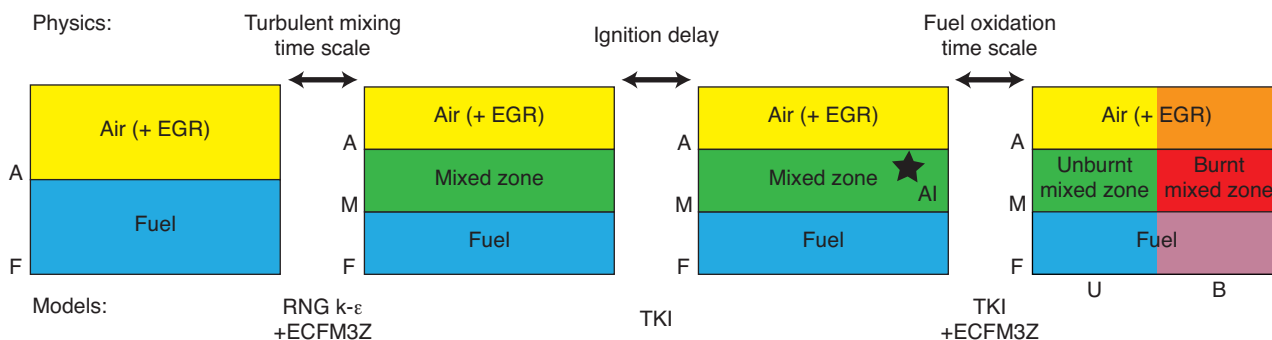


Figure 1

Scheme of the ECFM3Z combustion model workflow for compression-ignited operating points.

## 2.1 The Standard ECFM3Z Turbulent Combustion Model

ECFM3Z [14] is a sub-grid model aiming to describe the local in-cell mixing processes relevant to accurately predict the combustion and pollutant formation phenomena.

In order to represent the local mixing process, the ECFM3Z model includes a description of the local mixture stratification by considering three homogeneous sub-cell regions (see Fig. 1): one region contains only pure fuel (region F), the second region contains fresh air plus any additional EGR (region A) and the third region contains a mixture of the latter two (region M). During injection, the evaporation of the spray droplets leads to a source of mass in region F. The fuel and air (+EGR) from regions F and A turbulently mix to form region M. The characteristic mixing time  $\tau_m$  depends on the characteristic time scale of the turbulence. The mixture in region M may then auto-ignite. Auto-ignition can be handled by several specific models, here the TKI model, which provide an auto-ignition delay. When the auto-ignition delay is reached, combustion starts in region M, thereby dividing it into two zones: a fresh (or unburned) gas zone and a burnt gas zone. As the mixed fresh gases in region M are oxidised by auto-ignition, the hot products formed are added to the burnt gas mixing region. During combustion, the turbulent mixing leads to the addition of pure air (+EGR) and pure fuel (from the burnt gas part of region A and F, respectively) directly into the burnt gas part of the mixed region. The oxidation of this part of the injected fuel with the mechanism described below as the CORK model represents the diffusion flame.

## 2.2 The ECFM3Z-pdf Turbulent Combustion Model

In real mixtures, a pure air (+EGR) and a pure fuel region cannot be found. Instead, the mixture can be described as a continuous distribution of intermediate states between pure component states. This type of structure can be modelled by a probability density function (pdf) of the mixture fraction variable.

Calling this mixture fraction variable  $Z$ , the standard ECFM3Z model can be seen as a first stage approximation in which the pdf function is built only on three Dirac distributions:

$$P(Z) = a\delta(Z) + b\delta(Z - \bar{Z}^M) + c\delta(Z - 1)$$

The first delta function corresponds to the unmixed air region A, the second one to the mixed region M and the third one to the unmixed fuel region F. These regions are homogeneous reactors. Besides, the state of region M is only controlled by the mass flows from the fuel (F) and air (A) regions which are based on a turbulent time scale.

To improve the mixture formation modelling, the ECFM3Z-pdf model [15] has been created as an extension of

the standard ECFM3Z model. It relies on the addition of a probability density function to describe the in-cell mixture. The sub-cell regions are not homogeneous reactors anymore but a part of a continuous distribution of Fuel/Air equivalence ratios. The region M contains the part of the mixture that is in the flammability region. The region A contains the mixture that is too lean to react and the region F contains the mixture that is too rich to react. Furthermore, the addition of the probability density function induces a real mixing description which is able to model the sub-cell heterogeneities.

## 2.3 The TKI Model

To numerically study any compression-ignited combustion mode burning Diesel, an auto-ignition model adapted to hydrocarbon fuels is needed. Such a model has to provide the auto-ignition delay and an accurate description of the subsequent chemical reactions. Indeed, a precise knowledge of the reaction rates is needed to correctly predict the initial pressure rise during combustion since this is related to the engine noise level and becomes a more and more limiting factor. The latest version of the TKI auto-ignition model [16, 17] meets all these requirements.

The Tabulated Kinetics of Ignition (TKI) auto-ignition model relies on tabulated auto-ignition variables deduced from detailed chemistry calculations performed with the Senkin code, which is part of the Chemkin package. The detailed mechanism has been generated by the Département de Chimie Physique des Réactions (CNRS, Nancy) for mixtures of n-heptane and isooctane [19]. This mechanism contains about 400 species and 2000 reactions. The 3D model variables are calculated once and for all for a large range of initial thermodynamic conditions and are stored in lookup tables. The fresh (or unburned) gas quantities that are used as input parameters of the auto-ignition lookup tables are the fresh gas temperature, pressure, Fuel/Air equivalence ratio, the rate of dilution and the octane number ( $ON = 0$  for Diesel calculations).

Figure 2 shows an example of the temperature profile predicted by the TKI model and a comparison with the temperature profile computed with the detailed chemistry mechanism. In this example, the thermodynamic conditions lead to a first part of the combustion controlled by the cool flame. To represent this phenomenon, two auto-ignition variables are defined: the auto-ignition delay  $\tau$  and the portion  $C_1$  of fuel consumed by the cool flame. Then, main ignition modelling is based on reaction rates  $\omega_{c_k}$  tabulated as a function of a progress variable. When the thermodynamic conditions lead to the absence of the cool flame effect,  $C_1 = 0$  and the main ignition is directly described by the reaction rates  $\omega_{c_k}$  once the auto-ignition delay  $\tau$  is reached.

In internal combustion engines, mixture and thermodynamic conditions evolve with the piston motion. Consequently, all model variables extracted from the data-

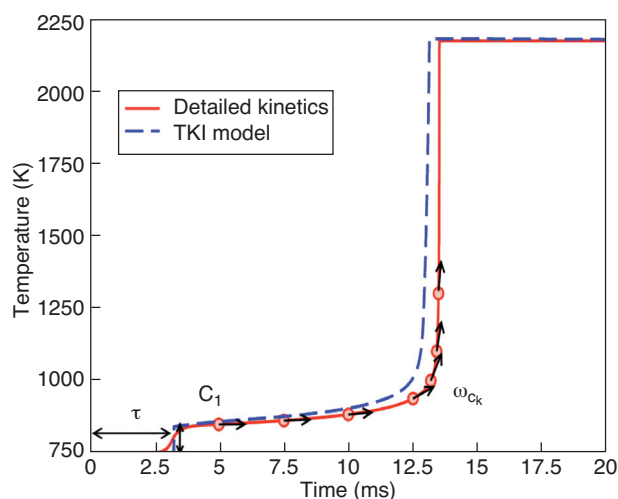


Figure 2

Comparison of temperature evolution from detailed kinetics and the TKI model for a constant volume reactor.

base vary (among them the delay  $\tau$ ). To take into account the evolution of  $\tau$ , a computation method taking into account the detailed kinetics and the mixture is necessary. For this purpose, a fictive species is considered to represent the time evolution from the onset of mixing until the delay is reached. The fictive species growth rate is proportional to the local fuel concentration and depends on the auto-ignition delay which varies with local thermodynamic conditions [16]. It is suitable to normalise the fictive species concentration with the fuel concentration so that the auto-ignition occurs when the fictive species concentration reaches one.

### 3 POLLUTANT MODELLING

Pollutant modelling occurs in the burnt gas part of the mixing region M. The burnt gases in region M might have two origins:

- The products due to the combustion in the unburned gases;
- Fuel and air coming from regions A and F due to turbulent mixing.

Consequently, the burnt gases in region M contain combustion products but also fuel and oxygen. Besides, burnt gases involve very high temperatures leading to diffusion combustion and pollutant formation (carbon monoxide, soot and nitrogen oxides).

The diffusion combustion and the formation of pollutants containing carbon can all be related to a global fuel oxidation path. The nitrogen oxides formation is treated as a separated

oxidation mechanism according to the Zeldovitch hypotheses. Details for these models are provided below.

#### 3.1 Modelling of Pollutants Containing Carbon Compounds

The main pollutants containing carbon compounds are carbon monoxide and soot particles. But there also exist traces of other species containing carbon compounds that are part of the chemical paths leading the formation of carbon monoxide, carbon dioxide and soot particles. Furthermore, evolving in-cylinder conditions may lead to incomplete combustion or oxidation that also produce unburned hydrocarbons. All phenomena are modelled considering a unique reaction path.

Figure 3 epitomises the reaction paths considered in the burnt gas part of region M. This set of chemistry reactions models the complex chemistry leading to the formation and oxidation of CO and soot. This structure results from the coupling of two formerly independent models [12]: the first one called CORK (CO Reduced Kinetics) is dedicated to CO modelling and the second one called PSK (Phenomenological Soot Kinetics [7]) is devoted to soot modelling.

The fuel oxidation in the burnt gas part of the mixing zone which leads to CO production and its oxidation into CO<sub>2</sub> is computed with a 6-step reduced kinetic model. This reduced 6-step kinetics is an improved version of the 4-step model of Hautman *et al.* [20] obtained by the addition of 2 extra chemical reactions in order to allow the coupling of this scheme with the PSK soot model. The reduced kinetics approach is justified by the fact that in ECFM3Z, the burnt gas side of the mixed zone, where high temperature combustion occurs, is considered as a homogeneous reactor. The model is applied on each computational cell where gas composition and temperature are conditioned in the burnt gas part of the mixing region of Figure 1.

The Hautman *et al.* 4-step model [20] can be applied to general hydrocarbons of the alkane family (C<sub>n</sub>H<sub>2n+2</sub>) and is described by Reactions R1.1 to R1.4. These reactions represent the fuel conversion into a general intermediate hydrocarbon – here assumed as ethylene (C<sub>2</sub>H<sub>4</sub>) –, the intermediate hydrocarbon oxidation into CO and H<sub>2</sub>, the CO oxidation into CO<sub>2</sub> and the H<sub>2</sub> oxidation into H<sub>2</sub>O, respectively. For the general intermediate hydrocarbon, the ethylene appears to be a good choice since it is present in large amounts in a number of larger hydrocarbon oxidation processes as shown for example in [19, 21–23]. The only important alteration of the original Hautman *et al.* model [20] is the consideration of reversibility for Reaction R1.3. This has to be added since at high temperature the dissociation of CO<sub>2</sub> into CO and O<sub>2</sub> becomes important. If not considered, the model would highly overestimate the final combustion temperature as well as the CO<sub>2</sub> concentration while the CO concentration would be underestimated. The reversibility was not considered in the original work of

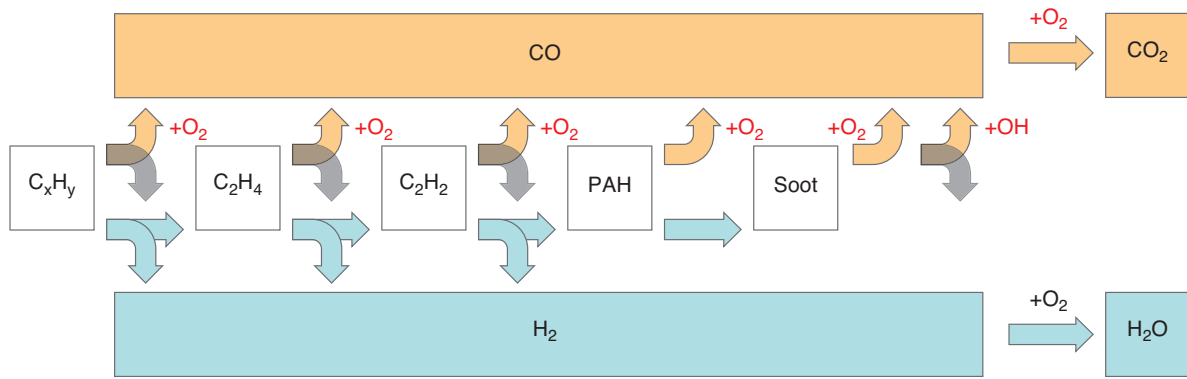
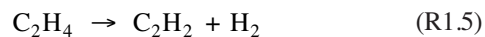
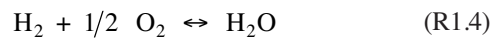
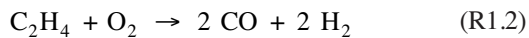
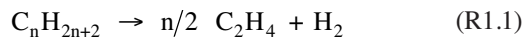


Figure 3

Scheme of the reaction paths for the carbon compounds in the burnt gas part of the mixing region (coupled PSK and CORK models).

Hautman *et al.* [20] because the model was tested in a temperature range where dissociation does not occur.

As the soot model needs to consider the acetylene ( $C_2H_2$ ) to build Polycyclic Aromatic Hydrocarbons (PAH), this species has to be added in the fuel conversion path, which leads to the addition of Reactions R1.5 and R1.6. These reactions represent the acetylene formation through ethylene conversion and the acetylene oxidation into CO and  $H_2$ , respectively.

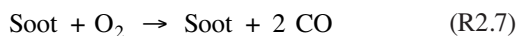
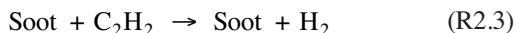
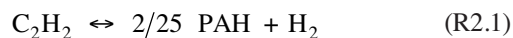


Beyond the more or less complete conversion of fuel into  $H_2O$  and  $CO_2$  following the 6-step mechanism, the formation and oxidation of soot particles have also to be considered. Soot models applied to Diesel combustion can be gathered into two classes, one based on the flamelet concept and the other based on the homogeneous reactor concept. The first assumes that the laminar diffusion flame structure of the reaction zone, in the mixture fraction space, is preserved while convected and strained by the turbulent flow. The second assumes that the properties of the reaction zone are locally homogeneous. Thus the aerodynamic and chemical reaction interactions are modelled with opposed assumptions: the first assumes fast chemistry, the second fast mixing.

To be coherent with the whole ECFM3Z model strategy, the homogeneous reactor concept is applied in the burnt gas part of the mixing region for soot modelling. In the original PSK model [7], the acetylene ( $C_2H_2$ ) production was directly obtained through fuel decomposition. When coupled with the CORK model, the  $C_2H_2$  is now indirectly produced based on fuel following Reaction R1.5. Similarly, the original PSK model contains oxidation reactions for  $C_2H_2$  and  $H_2$  which are now part of the CORK model. As a consequence, the original 11-step PSK model is reduced to a 8-step phenomenological model (Reactions R2.1 to R2.8) when coupled with the CORK model.

Reaction R2.1 is introduced to describe the complex polymerization process that leads to soot precursor (PAH) formation from acetylene. The PAH species is assumed to be  $C_{25}$  which is in agreement with recent measurements by mass spectrometry [24]. Based on PAH, soot is formed through soot inception (Reaction R2.2). But once soot is already present, soot particles may grow by acetylene and/or PAH addition as well as soot coagulation (Reactions R2.3, R2.4 and R2.5, respectively). This allows to account for various particle sizes. The oxidation sequence contains an oxidation reaction by  $O_2$  for PAH (Reaction R2.6) and soot oxidation reactions by both  $O_2$  and OH radical (Reactions R2.7 and R2.8, respectively).

Despite the fact that PAH and soot are assumed to contain only carbon atoms in the model, the formation enthalpy of these two species is taken into account. Indeed, analyses of particles emitted by engines have shown that both their structure and composition are complex: the mass fraction of carbon is less than 90% and H mass fraction is around 1% [25]. Values of formation enthalpy of aromatic components up to  $C_{150}H_{30}$  ( $H/C = 0.2$ ) found in the literature [26] show that the formation enthalpy of such graphitic substance is not negligible.



To improve the simulation accuracy the CORK and PSK models are fully coupled to the ECFM3Z combustion model by taking into account the species in the mass and energy balances. Moreover, since the time step of the 3D CFD engine code is often not coherent with the very small chemical characteristic time scales, a cell-by-cell subcycling procedure based on the smallest chemical time of Reactions R1.x and R2.x has been developed. This allows to ensure precision in the resolution of both sets of reactions while avoiding to consider extremely reduced time steps for all cells and models.

### 3.2 NO<sub>x</sub> Modelling

Most research on the chemical reactions of nitrogen has been motivated by the impact of nitrogen compounds emitted from combustion sources on the environment. In the combustion of “clean” fuels (fuels not containing nitrogen compounds), the oxidation of atmospheric nitrogen (N<sub>2</sub>) by the thermal mechanism is the major source of NO<sub>x</sub> emissions. Among the nitrogen oxides, nitric oxide (NO) is the main species emitted during a combustion process.

Based on these observations, the most widely used model for the prediction of nitrogen oxide emissions is the extended Zeldovitch model [27, 28] which is based on the 3 following assumptions:

- The atmospheric nitrogen is the source of NO<sub>x</sub> (Hypothesis 1);
- The thermal NO<sub>x</sub> formation reactions are decoupled from the fuel oxidation process because the NO<sub>x</sub> formation reactions are slow compared to the fuel oxidation reactions (Hypothesis 2);
- The major part of nitrogen oxides resulting from the formation and oxidation processes are NO molecules whence the modelling of all NO<sub>x</sub> emissions based only on this molecule (Hypothesis 3).

Assuming these hypotheses, the Zeldovitch model is restricted to 3 reactions. Note that these reactions are present

in all the detailed chemistry mechanisms related to thermal NO formation whatever their degree of refinement.



Reactions R3.1 to R3.3 involve the O and OH radicals, which are also involved in the fuel oxidation mechanism. Hence, if Hypothesis 2 was not assumed, it would be necessary to couple the thermal NO reactions to the reaction sequence describing the fuel oxidation. Thanks to Hypothesis 2, the NO formation rates are simply calculated assuming equilibrium values for the temperature and the concentrations of O<sub>2</sub>, N<sub>2</sub>, O and OH. The N atom concentration is calculated from a steady-state approximation applied to Reactions R3.1 to R3.3. The errors introduced by this approximation have been investigated in detail by Miller and Bowman in [29]. The non-equilibrium effects on the NO formation rate are observed on a wide temperature range but only during the initial stages of reaction which are only responsible for very little NO formation.

## 4 NOISE LEVEL COMPUTATION

The noise level is computed based on the mean in-cylinder pressure trace in order to mimic the analysis performed on the test bench. First, a spectral analysis of the pressure curve is performed. Then, a filter is applied to represent the attenuation due to an average engine block. The whole process provides a treatment equivalent to the AVL noisemeter.

## 5 HCCI AND LTC COMBUSTION MODES

The HCCI (Homogeneous Charge Compression Ignition) and LTC (Low Temperature Combustion) acronyms are the most commonly used to designate a wide category of innovative combustion modes intending to dramatically reduce the pollutant emissions with respect to the conventional Diesel combustion [1]. Their existence is based on the analysis of the local conditions leading to pollutant formation:

- NO<sub>x</sub> emissions are mainly related to local temperature (increasing emissions with increasing temperature) and secondly to Fuel/Air equivalence ratio (FAER) with highest emissions located between FAER = 0.7 and 1.2;
- Soot emissions are mainly related to local Fuel/Air equivalence ratio (increasing emissions with increasing FAER) and secondly to temperature. The effect of temperature is somewhat more complicated than for NO<sub>x</sub> emissions as a higher temperature promotes soot particle creation as well as their oxidation. Furthermore, the ever-evolving local

temperature in an internal combustion engine and the dominating influence of local mixture prevents from drawing general trends about temperature influence;

- CO emissions may be related to incomplete combustion due to bulk kinetics “freezing” or to incomplete combustion linked with a lack of oxygen in locally rich conditions but also to CO<sub>2</sub> dissociation at high temperature. Therefore, both high and low temperature as well as high and low Fuel/Air equivalence ratio may lead to important CO emissions.

Based on these considerations, the HCCI and LTC concepts tend to define operating conditions leading to favourable local conditions in order to prevent pollutant formation and quite more seldom to promote their conversion.

The HCCI concept as its name states relies on a homogeneous mixture in order to avoid the soot and CO formation processes related with locally rich mixtures existing in highly heterogeneous mixture. Furthermore, in order to limit the NO<sub>x</sub> formation, the homogeneous mixture should be relatively lean (FAER < 0.7) and cold (peak temperature below 1500 K). Such conditions may only be created in DI Diesel engines with early injections of a limited amount of fuel which has an unfavourable impact on the load range. Another drawback of the homogeneous mixture is the bulk combustion following the auto-ignition which produces a high pressure gradient and consequently unacceptable noise emissions. To limit the combustion temperature and the kinetically-controlled reaction rates of such mixtures, a massive dilution with cooled recirculated burnt gases is often used. By decreasing the local temperature and the local concentration in oxygen, the dilution tends to reduce the reaction rates and consequently the noise level as well as the NO<sub>x</sub> emissions. On the other hand, this can turn into a local lack of oxygen which impedes soot and CO oxidation and induces higher soot and CO emissions.

The LTC concept aims to approach the theoretical benefits of HCCI combustion mode while avoiding its drawbacks mainly related with the uncontrolled bulk combustion. The realisation of a relatively cold mixture with controlled reaction rates relies on the combination of a controlled dilution rate and a dedicated injection strategy. Adding flexibility with respect to the strict-sense HCCI combustion, the LTC concept allows to reach new trade-offs between Fuel/Air equivalence ratio and dilution rate by transferring a larger part of the control on the reaction rate and the local conditions to the injection strategy. Particularly, the prospected combustion is not necessarily a pure premixed kinetically-controlled combustion anymore but is rather a combination of premixed kinetically-controlled and diffusion mixing-controlled combustions. Contrary to conventional Diesel combustion, the amount of diffusion combustion is restricted to limit the soot particle formation. The LTC concept allows an extension of the operating range with respect to the strict-sense HCCI combustion mode but the restriction in terms of

diffusion combustion proportion and the use of dilution still induces a limitation in terms of higher possible load.

## 6 THE NADI™ CONCEPT

The NADI™ (Narrow Angle Direct Injection™) concept [30-33] is a combustion chamber design concept for Diesel engines whose aim is to improve the control of the mixture formation. Using a reduced spray angle with respect to conventional Diesel engines, it is able to cope with very early injections without fuel impingement on the cylinder liner while it acts as a wall-guided direct injection concept for injections phased near the TDC. The combination of the restricted spray angle with a dedicated piston bowl design allows to obtain with a unique chamber design the strict-sense HCCI combustion mode for the lowest loads, the LTC concept for mid loads and efficient conventional Diesel combustion at full load. The wall-guided mixture formation is particularly useful for the LTC concept because it improves the control on the cycle-to-cycle repeatability of the combustion. Nevertheless, because of its wall-guided mixture formation concept, the NADI™ injection strategies must be carefully selected to avoid any fuel film creation on the piston dome [33].

## 7 SELECTED OPERATING POINTS

One of the most important limitations of the HCCI/LTC concepts is the restricted operating range and the consequent strategy switch with conventional Diesel combustion near the higher load limit of this range that is located in the NEDC speed – load range. In this particular operating region, dilution is necessary to be able to continuously evolve towards pure HCCI/LTC operating points but has to be limited because of its negative impact on soot emissions. Additionally, the transition in dilution rate with increasing load and speed has also to be smooth to avoid operating points with high NO<sub>x</sub> emissions and/or noise level.

In such a context, the use of 3D CFD may be highly beneficial if predictive noise and pollutant emission computations may be realised. Indeed, 3D CFD may then be both instructive in order to understand the phenomena explaining the experimental results and useful to optimise the combustion chamber design or the injection strategy.

In the present work, the focus is set on operating points located near the higher load limit of the HCCI/LTC operating range of a NADI™ single-cylinder engine and on the peak power operating point. A first operating point (1500 rpm – 6.8 bar IMEP) is a relatively high load operating point in the HCCI/LTC operating range. Such an operating point has operating conditions selected to produce low soot and NO<sub>x</sub> emissions but suffers from a high noise level and a relatively low efficiency. The second operating point (2500 rpm –

9.5 bar IMEP) is located just outside the HCCI/LTC operating region which implies operating strategies typical of conventional Diesel combustion but with a certain amount of dilution to limit the  $\text{NO}_x$  emissions and to ease the transition in case of reducing load. The operating strategy constraints lead to an operating point producing both soot and  $\text{NO}_x$ , which imposes to define a trade-off between them that is not necessarily optimal in terms of noise emissions or efficiency. The third operating point is the peak power operating point. This operating point is not a difficulty in terms of dilution or injection strategy but is a *sine qua non* testing point as the definition of any low load optimised engine concept must have a restricted impact on the full load behaviour of the engine to be “commercially” acceptable.

## 8 MODELLED ENGINE

The modelled engine is a single-cylinder engine derived from a series Renault G9T 4-cylinder engine with a compression ratio reduced to 14.7:1 (see *Table 1*). A dedicated piston bowl profile typical of the NADI™ concept is used with an adapted injection angle. The injector is a series CRI 2.2 Bosch injector with 6 holes and a static mass flow rate of 450 ml/30 s/100 bar.

TABLE 1  
Main engine characteristics

Engine Type	Single-cylinder engine based on RENAULT G9T
Bore (mm)	87.0
Stroke (mm)	92.0
Compression ratio	14.7:1
Connecting Rod Length (mm)	149.9

## 9 OPERATING POINT 1: 1500 RPM – 6.8 BAR IMEP

This operating point is a “high load operating point” in the LTC region and has an important weight in the EUDC driving cycle making it a sensitive one. The selected operating conditions (see *Table 2*) are based on a high EGR rate in order to ensure low  $\text{NO}_x$  emissions ( $\sim 0.1$  g/kWh) and a pilot injection in order to limit as much as possible the noise level. The combination of a high EGR rate and the occurrence of diffusion reactions lead to soot emissions, especially for early injections. The selected variation is a sweep in injection timing (with a constant injection duration for each injection and a constant dwell between injections) to determine the best trade-off between noise level, soot emissions and efficiency.

The 3D CFD code is able to correctly reproduce the mean in-cylinder pressure evolution around TDC during the sweep

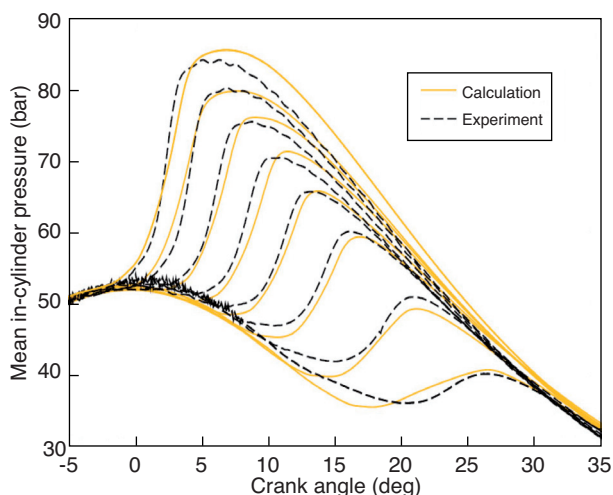


Figure 4

Pt #1 – Evolution of mean in-cylinder pressure during the injection timing sweep.

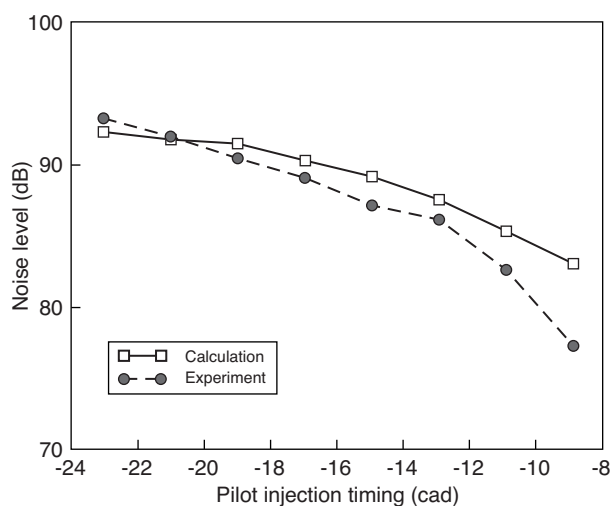


Figure 5

Pt #1 – Evolution of noise level during the injection timing sweep.

of injection timing (*Fig. 4*) which leads to a correct prediction of the noise level (*Fig. 5*). Nevertheless, the mean in-cylinder pressure is slightly overestimated during the expansion stroke which induces an overestimated power output and consequently an underestimated fuel consumption (*Fig. 6*). This is a problem when the aim is to compare different strategies in order to limit the fuel consumption penalty when lowering the pollutant emissions. For this operating point, the main difficulty in terms of pollutant emissions is the soot emissions whose evolution with injection timing is depicted

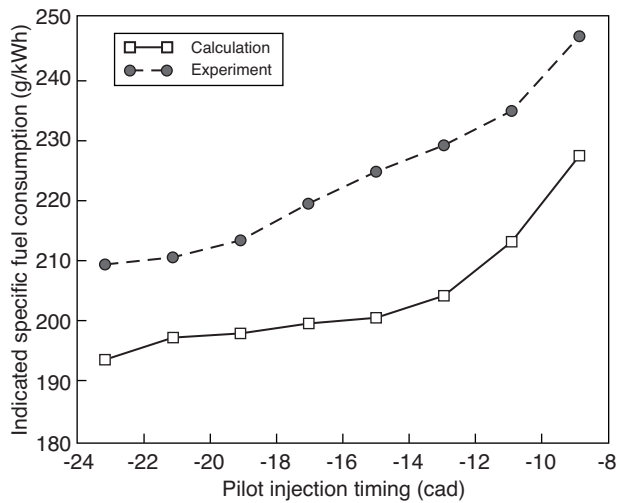


Figure 6

Pt #1 – Evolution of ISFC during the injection timing sweep.

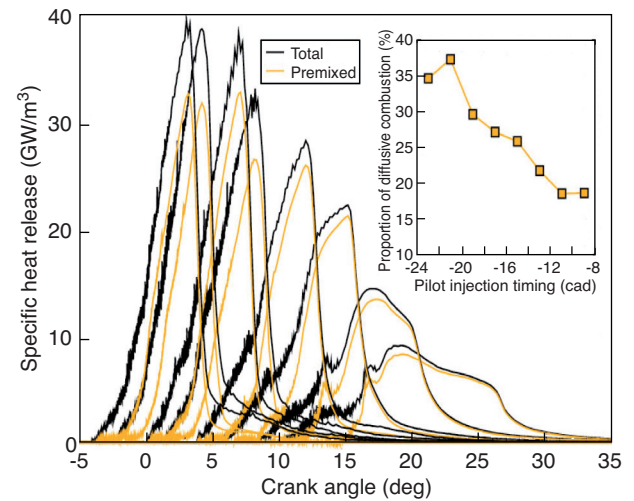


Figure 8

Pt #1 – Evolution of specific heat release and proportion of diffusion combustion (inserted diagram) during the injection timing sweep.

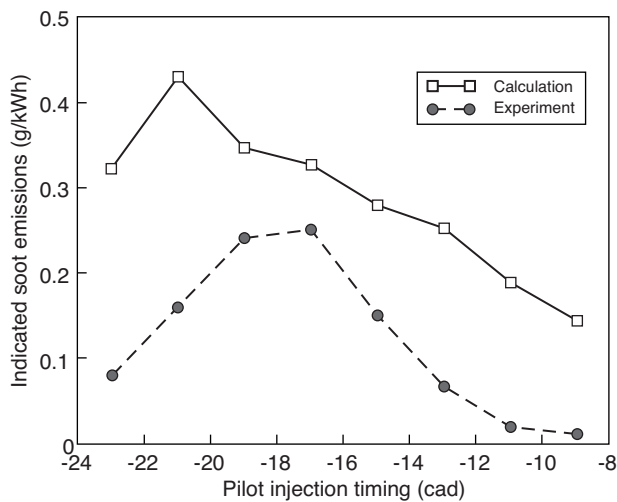


Figure 7

Pt #1 – Evolution of soot emissions during the injection timing sweep.

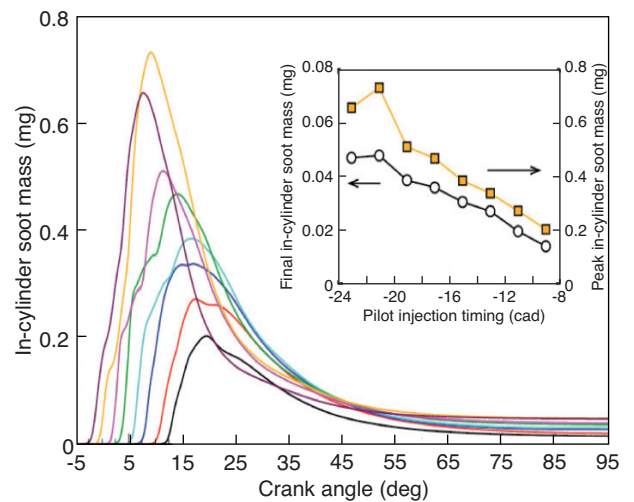


Figure 9

Pt #1 – Evolution of in-cylinder soot mass during the injection timing sweep.

in Figure 7. The trend depending on the injection timing is globally captured while the quantification of soot emissions is still a difficulty. The evolution of these emissions with the injection timing can be explained based on Figures 8 and 9.

First, Figure 8 indicates that, contrary to full load operating points, the combustion process is initially principally a diffusion combustion followed by a premixed combustion (see Figs. 10-13). The fact is that the auto-ignition occurs at the end of the injection process and first induces the oxida-

tion of the fuel coming from the later stages of injection (see Figs. 10, 11), hence the diffusion combustion. With later injection timings, the increase in auto-ignition delay leads to a relative decrease in the diffusion combustion proportion (see inserted diagram in Fig. 8). Figure 9 shows the crank-based evolution of the in-cylinder soot mass for all injection timings in the main diagram and the peak and final values in the secondary diagram. It is obvious that the final value is directly proportional to the peak one, meaning that the soot oxidation process during the expansion is quite similar for all

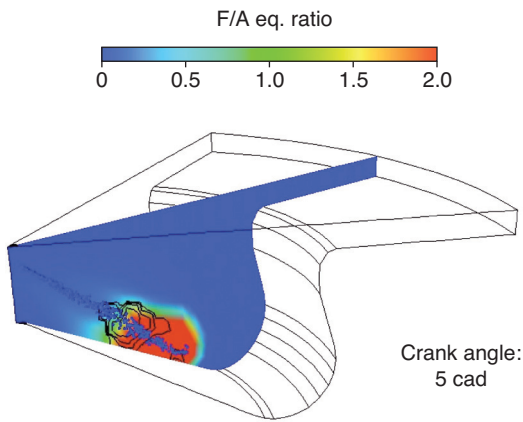


Figure 10  
Pt #1 – F/A eq. ratio field during the early diffusion phase (the black contour lines indicate the reaction area).

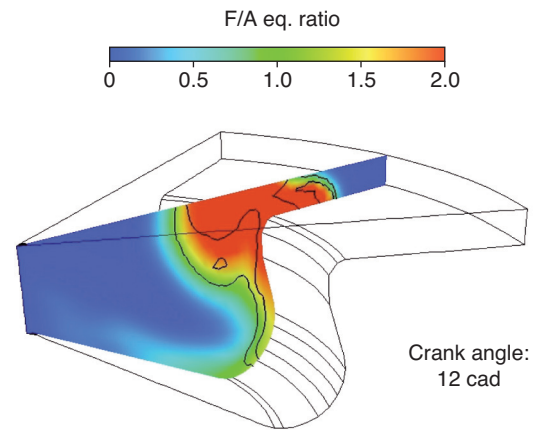


Figure 12  
Pt #1 – F/A eq. ratio field during the core of the premixed phase (the black contour lines indicate the reaction area).

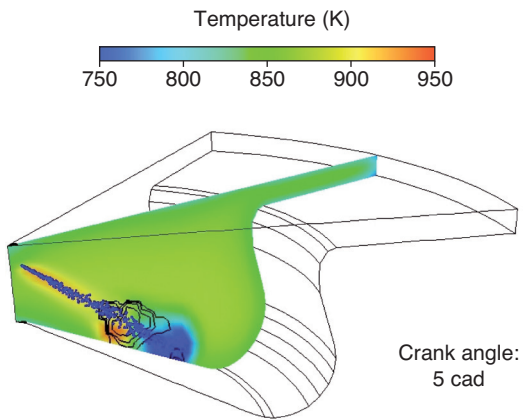


Figure 11  
Pt #1 – Temperature field during the early diffusion phase (the black contour lines indicate the reaction area).

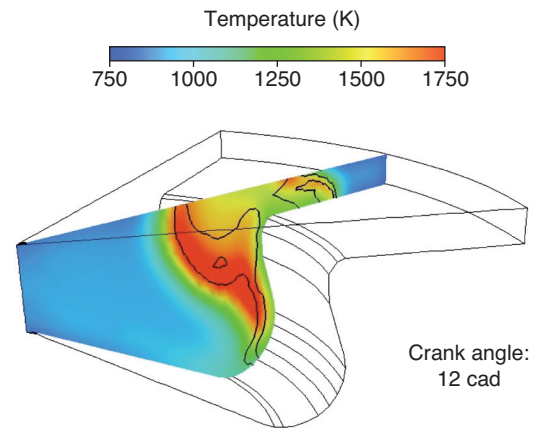


Figure 13  
Pt #1 – Temperature field during the core of the premixed phase (the black contour lines indicate the reaction area).

TABLE 2  
Pt #1 – Operating conditions

Engine speed (rpm)	1500
IMEP (bar)	target is 6.8
Intake pressure (bar)	1.50
Air mass flow rate (kg/h)	18.0
Fuel/Air equivalence ratio (-)	0.75
Exhaust Gas Recirculation (%)	about 44.0
Injection pressure (bar)	1370
Pilot injection timing (cad)	23.0 bTDC to 9.0 bTDC
Main injection timing (cad)	9.5 bTDC to 4.5 aTDC

injection timings. Furthermore, the comparison of the inserted diagrams in Figures 8 and 9 clearly indicates the dependency of the peak and final in-cylinder soot masses on the proportion of fuel that is burnt during the diffusion part of the combustion.

## 10 OPERATING POINT 2: 2500 RPM – 9.5 BAR IMEP

This operating point is just outside the LTC region but also has an important weight in the EUDC part of the driving cycle. Furthermore, its proximity with the LTC region

imposes to use strategies close to those used in the LTC region to ease the transition during transient operations (see Table 3).

For this operating point, the sweep in injection timing aims to define the best trade-off between the  $\text{NO}_x$  and the soot emissions. Once again the injection sweep is performed for a constant dwell between injections but the injection duration of the main injection is adapted to maintain a constant IMEP value.

The 3D CFD code appears to be able to represent quite well the IMEP as well as the pollutant emissions even if the computed IMEP is not perfectly constant contrary to the experimental measurements (Fig. 16). For carbon-containing pollutants, the trends are well reproduced even if the growth in CO (Fig. 17) and soot (Fig. 19) emissions for the latest injections is overestimated. For the  $\text{NO}_x$  emissions, the trend is perfectly reproduced but the quantification is about 40% too short (Fig. 18). Nevertheless, despite the defaults these results allow to identify the best trade-off operating conditions.

Contrary to the LTC operating point (1500 rpm – 6.8 bar IMEP), the combustion progress for this restricted dilution rate operating point is more conventional with four distinct parts (Fig. 15):

- The pilot injection is burnt by pure premixed combustion (see Figs. 20, 21);
- The early part of the main injection combustion is mainly premixed combustion;
- The main part of the main injection combustion is controlled diffusion combustion;

- The latest stage of the main injection combustion during early expansion is uncontrolled diffusion combustion.

This highly complex mix of combustion phases is due to the combination of the operating conditions and the injection strategy and explains the difficulty to accurately predict the mean in-cylinder pressure evolution (Fig. 14) and the pollutant emissions (Figs. 17-19). For argument's sake, the transition between the premixed and diffusion combustions of the main injection is depicted in Figures 22 and 23. There are simultaneously diffusion reactions at the fuel spray tip and premixed reactions at the bottom of the piston bowl. Furthermore, the 3D CFD results also underline the heavily heterogeneous mixture during such operation.

TABLE 3  
Pt #2 – Operating conditions

Engine speed (rpm)	2500
IMEP (bar)	9.5
Intake pressure (bar)	1.56
Air mass flow rate (kg/h)	50.0
Fuel/Air equivalence ratio (-)	0.69 to 0.79
Exhaust Gas Recirculation (%)	11.0
Injection pressure (bar)	1200
Pilot injection timing (cad)	28.0 bTDC to 18.0 bTDC
Main injection timing (cad)	10.0 bTDC to TDC

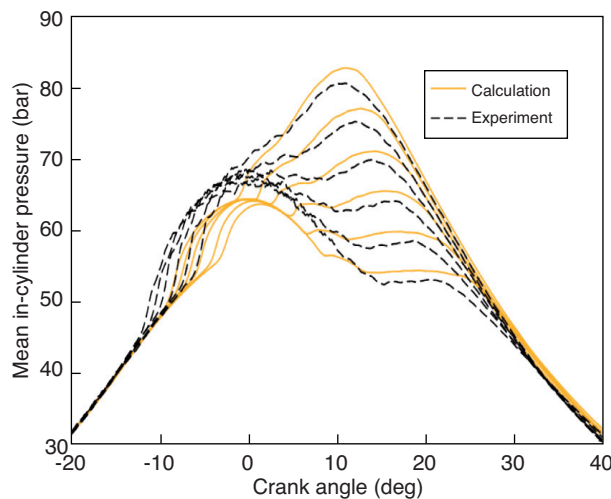


Figure 14

Pt #2 – Evolution of mean in-cylinder pressure during the injection timing sweep.

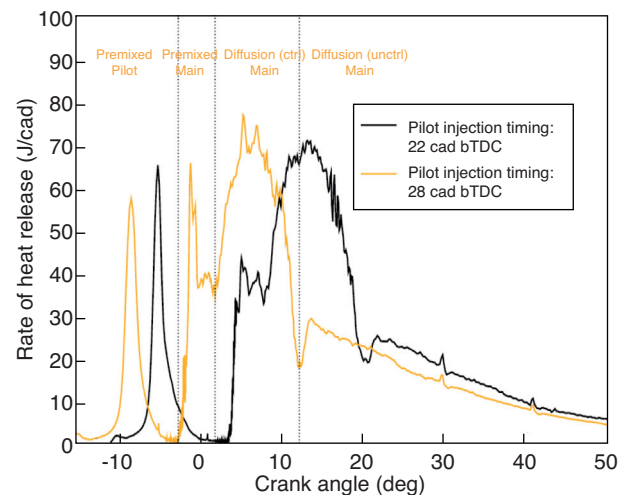


Figure 15

Pt #2 – Evolution of the heat release history for two injection timings.

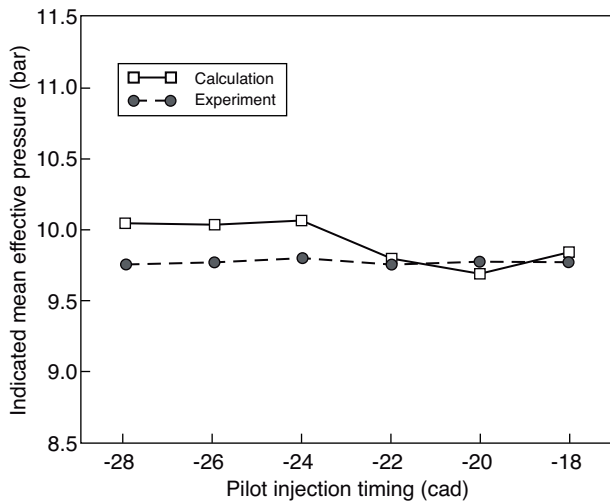


Figure 16

Pt #2 – Evolution of IMEP during the injection timing sweep.

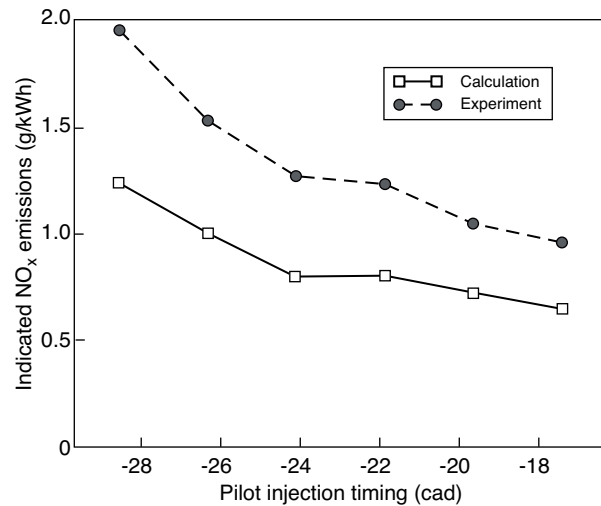


Figure 18

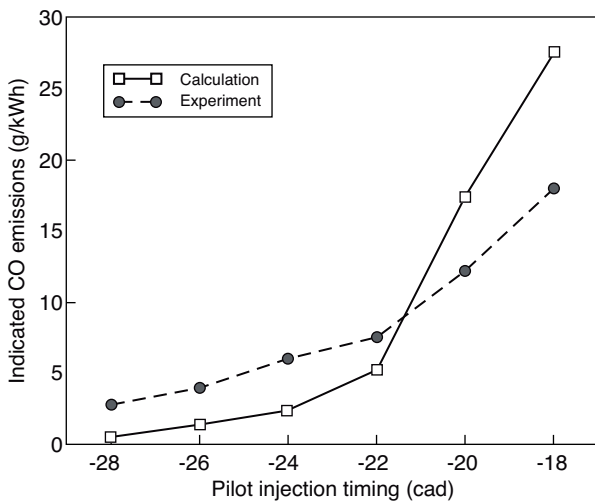
Pt #2 – Evolution of NO<sub>x</sub> emissions during the injection timing sweep.

Figure 17

Pt #2 – Evolution of CO emissions during the injection timing sweep.

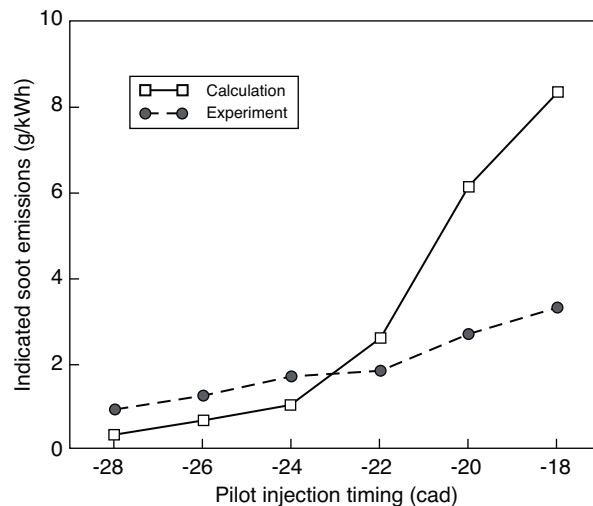


Figure 19

Pt #2 – Evolution of soot emissions during the injection timing sweep.

## 11 OPERATING POINT 3: 4000 RPM – FULL LOAD

For the peak engine power operating point, the considered variation is the traditional fuel enrichment in order to determine the highest acceptable Fuel/Air equivalence ratio for a given soot emission limit (see Table 4 and Fig. 24). The main demands concerning the numerical results are focused on the prediction of IMEP and soot emissions; the latter to be able to accurately define the highest Fuel/Air equivalence ratio, the former to directly compare various piston bowl designs in terms of power output.

As shown in Figure 25, the increase in power output with longer injection durations is quite well reproduced as well as the increase in carbon monoxide (Fig. 28) and soot emissions (Fig. 26). The decrease in NO<sub>x</sub> emissions is also captured even if the slope is a bit underestimated (Fig. 27). This pollutant is not critical for the present operating point but the considered variation is very useful to validate its modelling.

For the two most extreme injection durations, the heat release history and the evolutions of the in-cylinder pollutant masses are depicted in Figures 29-32, respectively.

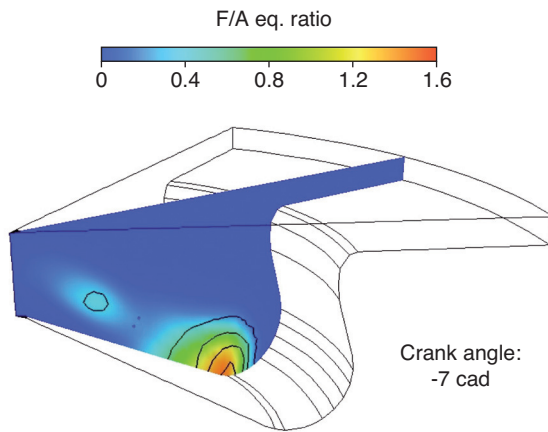


Figure 20

Pt #2 – F/A eq. ratio field during the pilot injection combustion (the black contour lines indicate the reaction area).

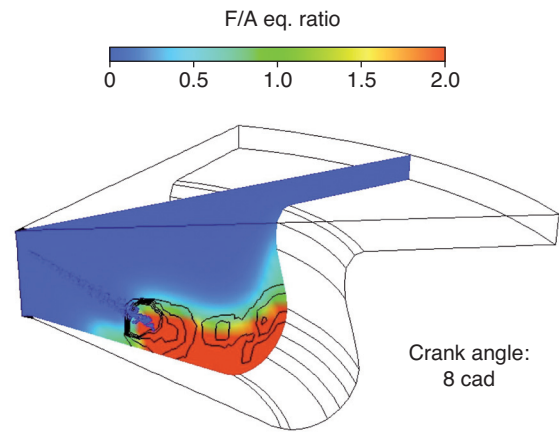


Figure 22

Pt #2 – F/A eq. ratio field at the transition between premixed and diffusion combustions for the main injection (the black contour lines indicate the reaction area).

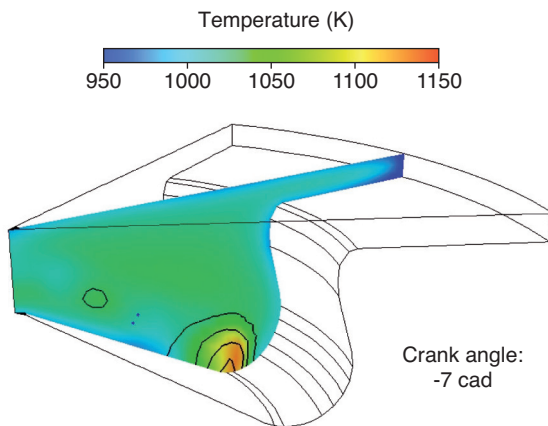


Figure 21

Pt #2 – Temperature field during the pilot injection combustion (the black contour lines indicate the reaction area).

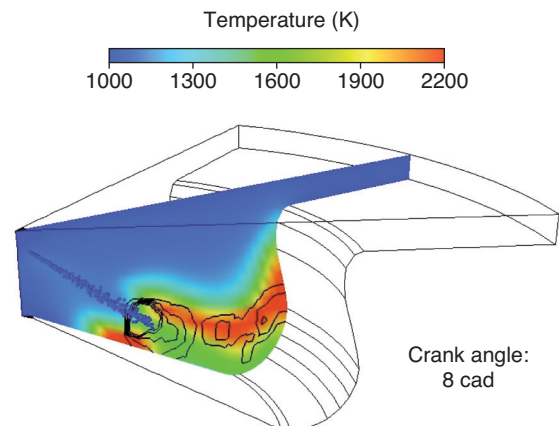


Figure 23

Pt #2 – Temperature field at the transition between premixed and diffusion combustions for the main injection (the black contour lines indicate the reaction area).

The combustion may be basically divided in three consecutive stages: a premixed combustion following the auto-ignition occurrence, a first part of diffusion combustion controlled by the injection process, ending approximately at the end of injection (EOI in the figures) and a second part of diffusion combustion that is uncontrolled. The evolution of the instantaneous in-cylinder mass for each pollutant may also be related to these three stages. There is no soot production during the premixed combustion but a net soot production during the controlled diffusion combustion

and a net soot oxidation during the uncontrolled diffusion combustion (Fig. 30). For the  $\text{NO}_x$  (Fig. 31), both the premixed combustion and the controlled diffusion combustion induce a net formation while the amount of  $\text{NO}_x$  is approximately stationary during the whole uncontrolled diffusion combustion. Carbon monoxide (Fig. 32) is produced both during the premixed and the controlled diffusion combustions while there is a net oxidation during the uncontrolled diffusion combustion. Furthermore, the rate of CO production appears to be higher during the premixed combustion.

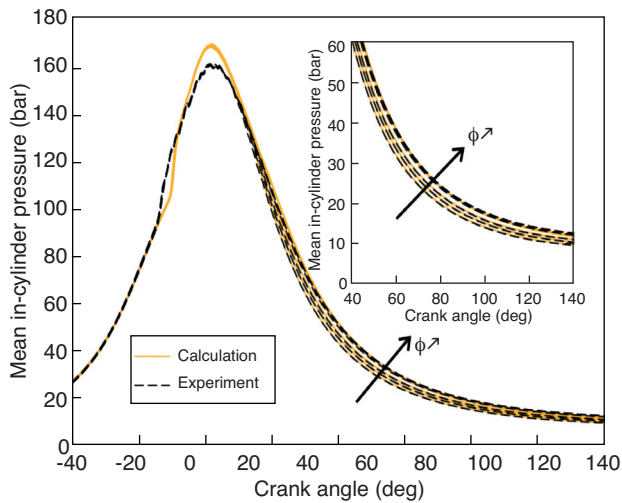


Figure 24

Pt #3 – Evolution of mean in-cylinder pressure trace with fuel enrichment ( $\phi$  symbolises fuel/air equivalence ratio).

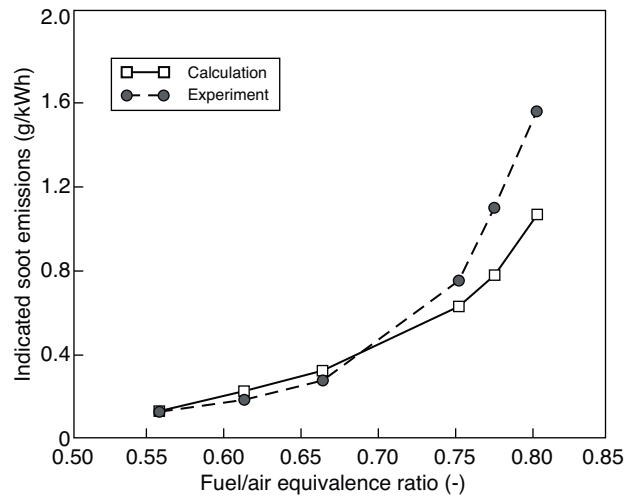


Figure 26

Pt #3 – Evolution of soot emissions with increasing Fuel/Air equivalence ratio.

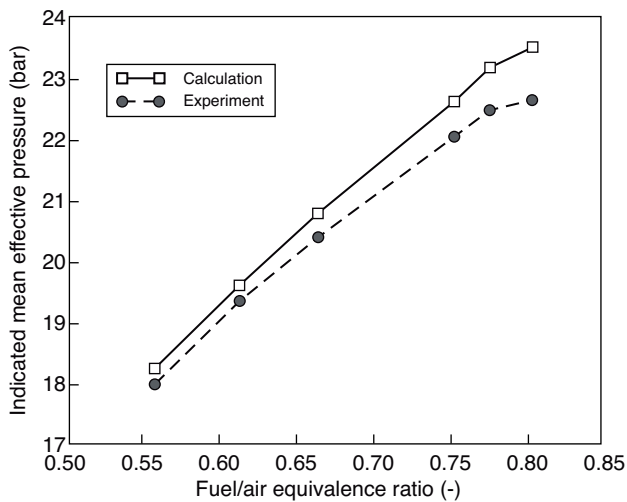


Figure 25

Pt #3 – Evolution of IMEP with increasing Fuel/Air equivalence ratio.

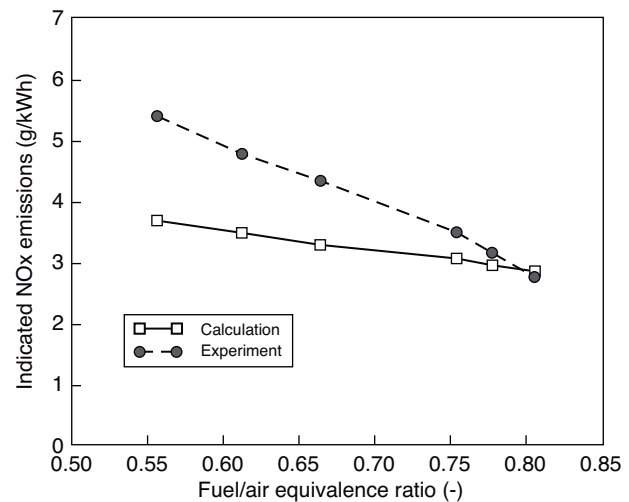


Figure 27

Pt #3 – Evolution of  $\text{NO}_x$  emissions with increasing Fuel/Air equivalence ratio.

The location of the soot and  $\text{NO}_x$  during the diffusion combustion may be related to the local FAER and temperature fields as indicated in Figures 33-36. The soot formation takes place in the rich burning areas at the spray tip while the  $\text{NO}_x$  are formed in the hot products resulting from the previous stages of the combustion.

The evolutions depicted in Figures 29 to 32 help to explain the measured trends in terms of engine-out emissions. First, the decrease in specific  $\text{NO}_x$  emissions (Fig. 27)

with increasing Fuel/Air equivalence ratio is not due to a change in the amount of  $\text{NO}_x$  that are produced during the combustion (masses are almost identical at EVO for both FAER in Fig. 31). Instead, the increase in in-cylinder  $\text{NO}_x$  mass with longer injections is quite moderate and inferior to the increase in power output. As a result, the indicated specific  $\text{NO}_x$  emissions are lower and lower with higher injected masses as long as the combustion is efficient enough to produce an important increase in power output

TABLE 4  
Pt #3 – Operating conditions

Engine speed (rpm)	4000
IMEP (bar)	17.0 to 22.0
Intake pressure (bar)	2.85
Air mass flow rate (kg/h)	164.0
Fuel/Air equivalence ratio (-)	0.56 to 0.81
Injection pressure (bar)	1600
Main injection timing (cad)	26.0 bTD

when the injected mass is increased. Second, the increases in soot (Fig. 26) and CO (Fig. 28) emissions with increasing Fuel/Air equivalence ratio are related to both a higher net production during the controlled diffusion combustion (because this period is longer while the rate of production is unchanged) and a shorter and less efficient net oxidation during the uncontrolled diffusion combustion. The increases in pollutant masses being this time far larger than the gain in power output, the indicated specific CO and soot emissions become worse and worse.

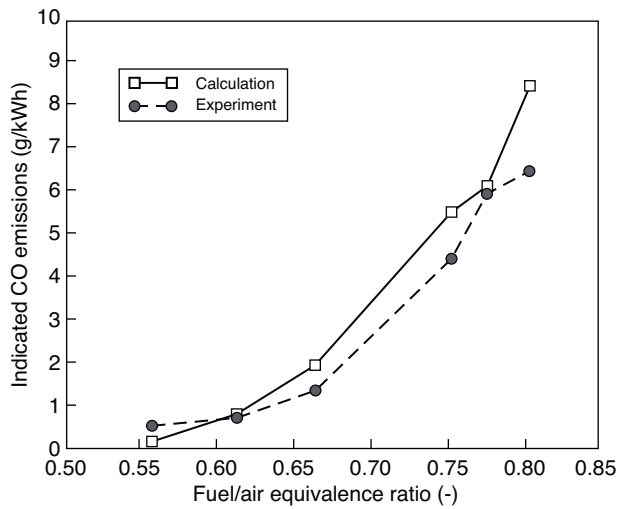


Figure 28

Pt #3 – Evolution of CO emissions with increasing Fuel/Air equivalence ratio.

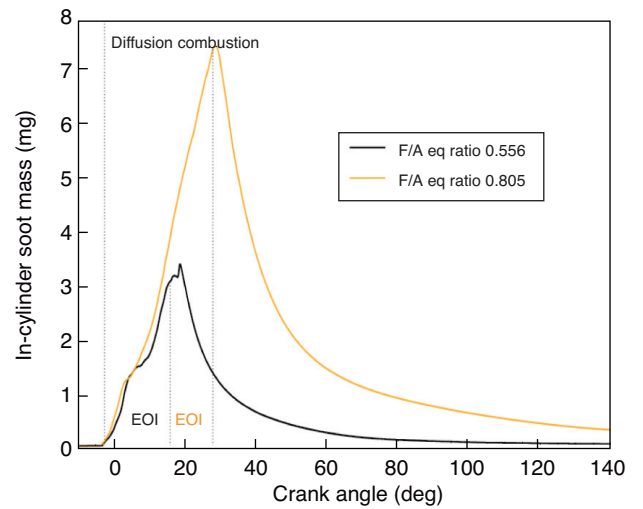


Figure 30

Pt #3 – Evolution of in-cylinder soot mass with crank angle for two F/A eq. ratios.

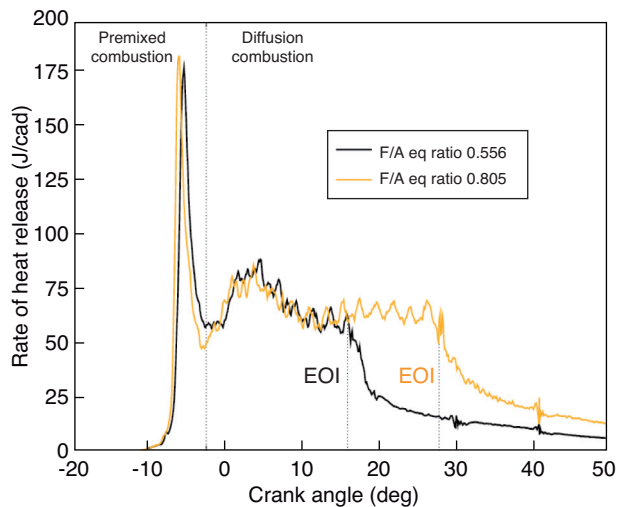


Figure 29

Pt #3 – Evolution of the rate of heat release with crank angle for two F/A eq. ratios.

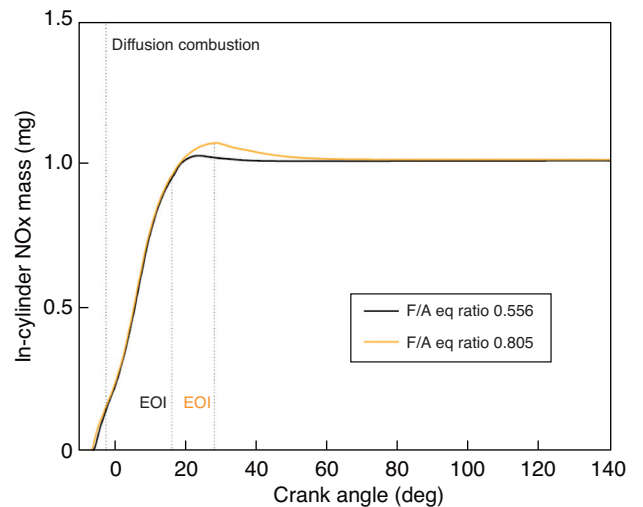


Figure 31

Pt #3 – Evolution of in-cylinder NO<sub>x</sub> mass with crank angle for two F/A eq. ratios.

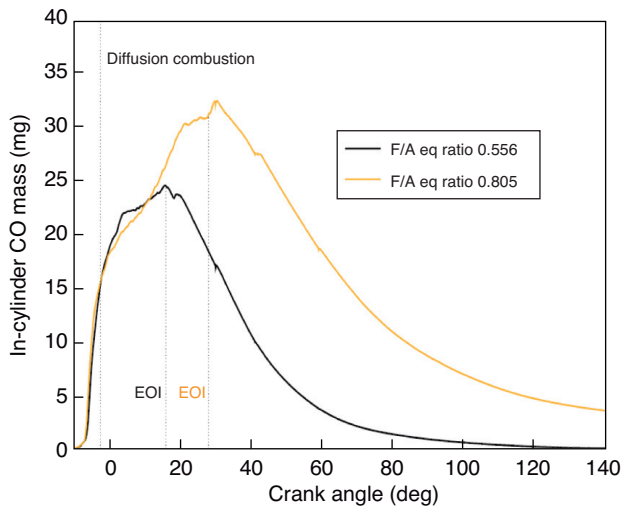


Figure 32

Pt #3 – Evolution of in-cylinder CO mass with crank angle for two F/A eq. ratios.

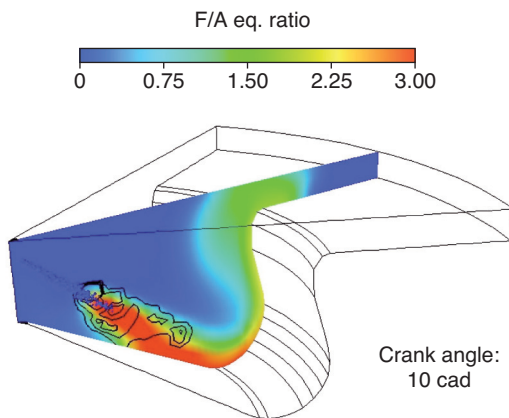


Figure 33

Pt #3 – F/A eq. ratio field at the transition between premixed and diffusion combustions for the main injection (the black contour lines indicate the reaction area).

## 12 PISTON BOWL DESIGN OPTIMISATION

Having combustion and pollutant models that provide reliable numbers on a major part of the engine map allows to use the 3D CFD tool in order to optimise the combustion chamber design from a global point of view. An example of the typical results that such an optimisation work provides is described in Figures 38 to 40 for three different piston bowl designs (Fig. 37).

These results are the relative variation of four quantities (IMEP, soot emissions,  $\text{NO}_x$  emissions and noise level) with

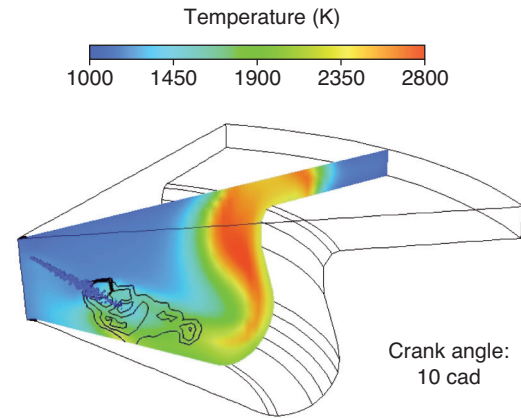


Figure 34

Pt #3 – Temperature field at the transition between premixed and diffusion combustions for the main injection (the black contour lines indicate the reaction area).

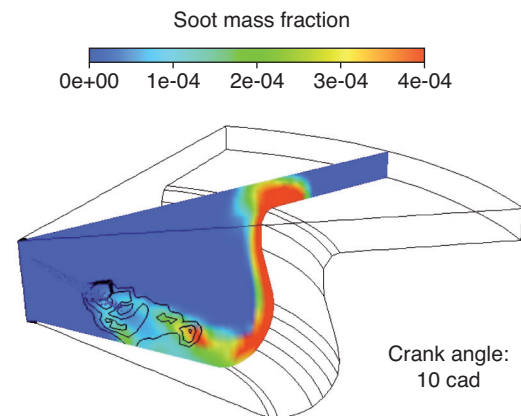


Figure 35

Pt #3 – Soot mass fraction field at the transition between premixed and diffusion combustions for the main injection (the black contour lines indicate the reaction area).

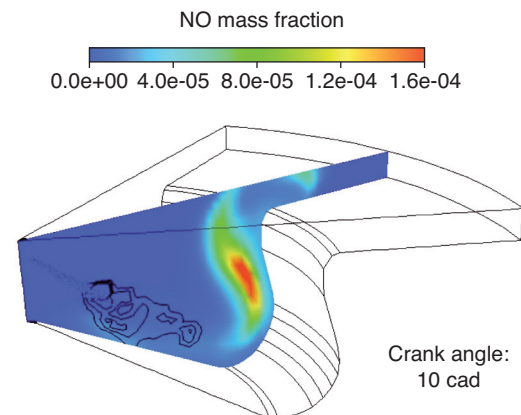


Figure 36

Pt #3 –  $\text{NO}$  mass fraction field at the transition between premixed and diffusion combustions for the main injection (the black contour lines indicate the reaction area).

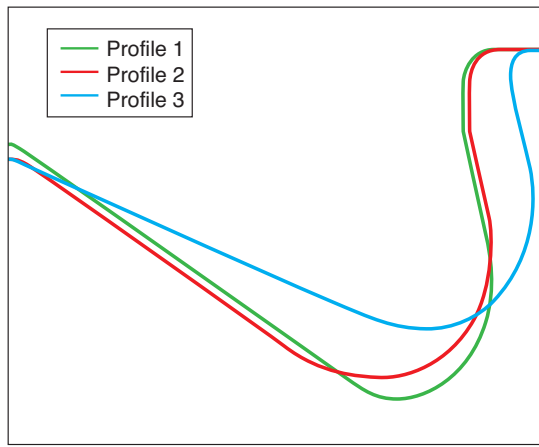


Figure 37  
Piston bowl profiles.

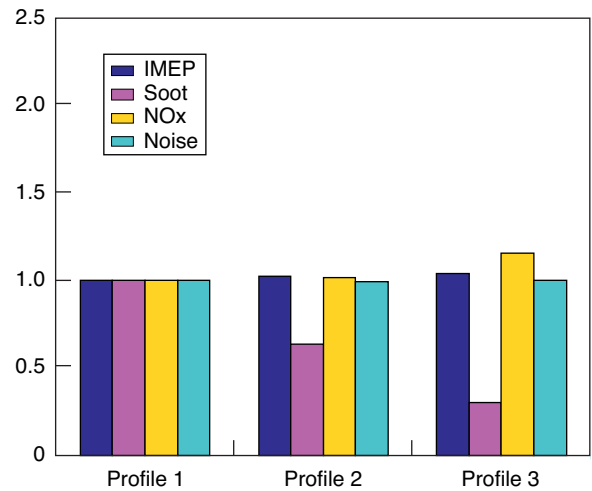


Figure 39  
Relative results at 2500 rpm – 9.5 bar IMEP.

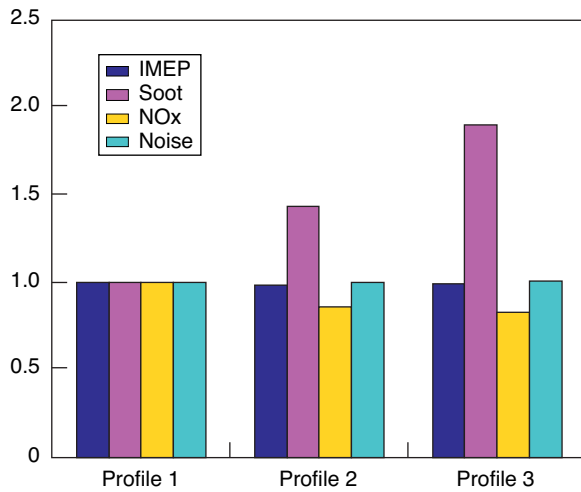


Figure 38  
Relative results at 1500 rpm – 6.8 bar IMEP.

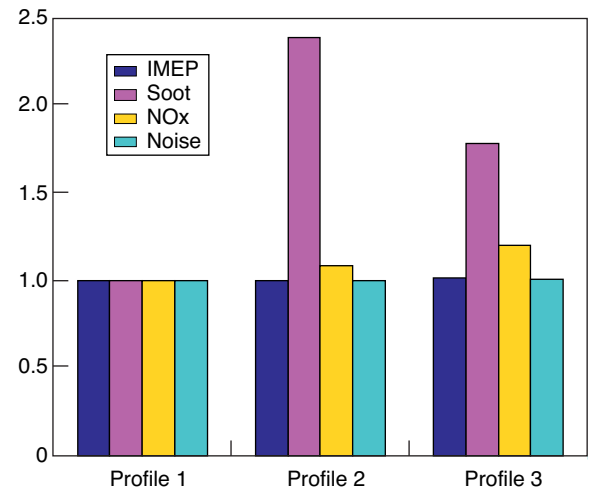


Figure 40  
Relative results at 4000 rpm – full load.

respect to their values for the first piston profile for a unique set of operating conditions for each operating point. This means that, in the present results, there is no adaptation of the engine settings when shifting from one piston profile to another to reach any predefined performances or emissions.

These results clearly show that a local optimisation of the piston bowl design is not an effective way to work because there is no simple and straightforward link between the design choices and the evolution of the pollutant emissions that is valid for all operating points. In such a context, the use of locally fitted pollutant models is therefore not possible as

they will be unable to provide the global information on the whole engine map.

On the other hand, quantitative pollutant modelling is needed for real life optimisation as the goal is not to compare the piston bowl designs on a unique set of engine settings but instead to compare the piston bowl performances with operating conditions dedicated for each design based on predefined constraints. For example, the piston bowl designs will be compared at 4000 rpm – full load based on IMEP considering a soot emission limit not to overcome. Therefore, quantitative soot emission prediction is necessary to find the highest realisable

load that respects the soot constraint for each piston bowl. Another example is the 2500 rpm – 9.5 bar IMEP operating point for which the EGR rate should be adapted to maintain the  $\text{NO}_x$  level constant and the piston profile selection based on the efficiency and the soot emissions.

Finally, the precise combustion and pollutant modelling provides very detailed information about the phenomena inducing the variations in engine efficiency and emissions that can be used to create new chamber design concepts or operating strategies.

## CONCLUSION

Recent model developments in the field of 3D CFD aim to switch from qualitative pollutant modelling (trend prediction) to quantitative pollutant modelling (providing reliable numbers). In such a context, the various pollutant models available in IFP-C3D have been constantly updated in parallel to combustion modelling improvements. The present versions of the CORK, PSK and Extended Zeldovitch models are a step forward in this quest concerning modelling of carbon monoxide, soot particles and nitrogen oxides, respectively. These models have already been applied to numerous engine configurations and have shown improved prediction capabilities while not penalising the CPU time consumption.

In the field of LTC engine concepts, and more particularly of the NADI™ concept, the continuous improvement of the combustion and pollutant modelling allows to gain a deeper and deeper knowledge of the engine behaviour. Furthermore, the quantitative prediction of pollutants with models valid for the whole engine operating range gives room for more complete chamber design optimisation. Indeed, a chamber design optimisation of some particular operating points, with the aim not to impede too much the performances and emissions on others, becomes now possible.

The constant improvement of the accuracy for combustion and pollutant modelling with the 3D CFD tool for the closed valve part of the cycle makes more and more obvious the necessity to compute the whole engine cycle as well as the after-treatment devices in a numerically effective way to fully benefit from the generated information. Present work about 1D and 3D CFD coupling in various parts of the engine system (induction, injection, combustion, exhaust, after-treatment, ...) is a very promising answer.

## REFERENCES

- 1 Strangmaier R.H., Roberts C.E. (1999) Homogeneous Charge Compression Ignition (HCCI): Benefits, Compromises and Future Engine Applications, *SAE Paper* 1999-01-3682.
- 2 Barths H., Antony C., Peters N. (1998) Three-dimensional Simulation of Pollutant Formation in a DI Diesel Engine Using Multiple Interactive Flamelets, *SAE Paper* 982459.
- 3 Barths H., Pitsch H., Peters N. (1999) Three-dimensional Simulation of DI Diesel Combustion and Pollutant Formation Using a Two-component Reference Fuel, *Oil Gas Sci. Technol.* **54**, 233-244.
- 4 Kong S.C., Reitz R.D. (2003) Application of Detailed Chemistry and CFD for Predicting Direct Injection HCCI Engine Combustion and Emissions, *Proceedings of 29th International Symposium on Combustion* **29**, 1, 663-669.
- 5 Gopalakrishnan V., Abraham J. (2004) Computed NO and Soot Distribution in Turbulent Transient Jets under Diesel Conditions, *Combust. Sci. Technol.* **176**, 603-641.
- 6 Huguet C., Millet C.-N., Menegazzi P., Martin B., Chaumeix N., Paillard C.E. (2005) Correlation between Kinetic Reactivity and Structural Changes for Catalytic and Non-catalytic Oxidation of Diesel Soot, *European Combustion Meeting*.
- 7 Martinot S., Béard P., Roesler J., Garo A. (2001) Comparison and Coupling of Homogeneous Reactor and Flamelet Library Soot Modeling Approaches for Diesel Combustion, *SAE Paper* 2001-01-3684.
- 8 Patterson M.A., Kong S.C., Hampson G.J., Reitz R.D. (1994) Modeling the Effects of Fuel Injection Characteristics on Diesel Engine Soot and  $\text{NO}_x$  Emissions, *SAE Paper* 940523.
- 9 Smooke M.D., Long M.B., Connelly B.C., Colket M.B., Hall R.J. (2005) Soot Formation in Laminar Diffusion Flames, *Combust. Flame* **143**, 613-628.
- 10 Tao F., Golovitchev V.I., Chomak J. (2004) A Phenomenological Model for the Prediction of Soot Formation in Diesel Spray Combustion, *Combust. Flame* **136**, 270-282.
- 11 Kazakov A., Foster D.E. (1998) Modeling of Soot Formation during DI Diesel Combustion Using a Multi-step Phenomenological Model, *SAE Paper* 982463.
- 12 Jay S., Béard P., Pires da Cruz A. (2007) Modeling Coupled Processes of CO and Soot Formation and Oxidation for Conventional and HCCI Diesel Combustion, *SAE Paper* 2007-01-0162.
- 13 Zolver M., Klahr D., Bohbot J., Laget O., Torres A. (2003) Reactive CFD in Engines with a New Unstructured Parallel Solver, *Oil Gas Sci. Technol.* **58**, 33-46.
- 14 Colin O., Benkenida A. (2004) The 3-Zones Extended Coherent Flame Model (ECFM3Z) for Computing Premixed/Diffusion Combustion, *Oil Gas Sci. Technol.* **59**, 593-609.
- 15 Colin O. (2007) Étude GSM D.C.1 2006 – Modélisation Diesel, Phase 1 : Amélioration du modèle de mélange dans ECFM3Z, *Rapport IFP* 59798.
- 16 Colin O., Pires da Cruz A., Jay S. (2005) Detailed Chemistry Based Auto-ignition Model Including Low Temperature Phenomena Applied to 3-D Engine Calculations, *Proceedings of the Combustion Institute* **30**, 2649-2656.
- 17 Knop V., Jay S. (2006) Latest Developments in Gasoline Auto-ignition Modelling Applied to an Optical CAI™ Engine, *Oil Gas Sci. Technol.* **61**, 121-138.
- 18 Béard P. (2005) Towards a Predictive Modeling of Transient Injection Conditions of Diesel Sprays in DID Engines, *Proceedings of the ILASS Americas 18th Annual conference*.
- 19 Buda F., Bounaceur R., Warth V., Glaude P.A., Fournet R., Battin-Leclerc F. (2005) Progress Toward a Unified Detailed Kinetic Model for the Auto-ignition of Alkanes from C4 to C10 between 600 and 1200 K, *Combust. Flame* **142**, 170-186.
- 20 Hautman D.J., Dryer F.L., Schug K.P., Glassman I. (1981) A Multiple-step Overall Kinetic Mechanism for the Oxidation of Hydrocarbons, *Combust. Sci. Technol.* **25**, 219-235.
- 21 Warnatz J. (1984) Chemistry of High Temperature Oxidation of Alkanes up to Octane, *Twentieth Symposium (International) on Combustion*, The Combustion Institute, pp. 845-856.

- 22 Curran H.J., Gaffuri P., Pitz W.J., Westbrook C.K. (1998) A Comprehensive Modeling Study of n-heptane Oxidation, *Combust. Flame* **114**, 149-177.
- 23 Westbrook C.K. (2000) Chemical Kinetics of Hydrocarbon Ignition in Practical Combustion Systems, *Twenty-eight Symposium (International) on Combustion*, The Combustion Institute, pp. 1563-1577.
- 24 Dobbins R.A., Fletcher R.A., Benner B.A., Hoefft S. (2006) Polycyclic Aromatic Hydrocarbons in Flames, in Diesel Fuels and in Diesel Emissions, *Combust. Flame* **144**, 773-781.
- 25 Collura S., Chaoui N., Koch A., Weber J.V. (2003) Diesel Soot Combustion: Influence of the Amount of Soluble Organic Fraction on the Kinetic Parameters, *New Carbon Materials* **18**.
- 26 Wang H. (1992) Detailed Kinetic Modeling of Soot Particle Formation in Laminar Premixed Hydrocarbon Flames, *PhD Thesis*, Pennsylvania State Univ., USA.
- 27 Heywood J.B. (1988) *Internal Combustion Engine Fundamentals*, Mc Graw Hill.
- 28 Zeldovitch YA.B., Sadovnikov P.YA., Frank-Kamenetskii D.A. (1947) *Oxidation of Nitrogen in Combustion*, translated by Shelef M., Academy of Science of USSR, Moscow.
- 29 Miller J.A., Bowman C.T. (1989) Mechanism and Modeling of Nitrogen Chemistry in Combustion, *Prog. Energ. Combust.* **15**, 287-338.
- 30 Walter B., Gatellier B. (2002) Development of the High Power NADI™ Concept Using Dual Mode Diesel Combustion to Achieve Zero NO<sub>x</sub> and Particulate Emissions, *SAE Paper 2002-01-1744*.
- 31 Walter B., Gatellier B. (2003) Near Zero NO<sub>x</sub> Emissions and High Fuel Efficiency Diesel Engine : the NADI™ Concept Using Dual Mode Diesel Combustion, *Oil Gas Sci. Technol.* **58**, 101-114.
- 32 Ranini A., Potteau S., Gatellier B. (2004) New Developments of the NADI™ Concept to Improve Operating Range, Exhaust Emissions and Noise, *THIESEL 2004 Conference on Thermo- and Fluid Dynamic Processes in Diesel Engines*, Valence.
- 33 Réveillé B., Kleemann A., Knop V., Habchi C. (2006) Potential of Narrow Angle Direct Injection Diesel Engines for Clean Combustion: 3D CFD Analysis, *SAE Paper 2006-01-1365*.

*Final manuscript received in April 2008  
Published online in June 2008*

Copyright © 2008 Institut français du pétrole

Permission to make digital or hard copies of part or all of this work for personal or classroom use is granted without fee provided that copies are not made or distributed for profit or commercial advantage and that copies bear this notice and the full citation on the first page. Copyrights for components of this work owned by others than IFP must be honored. Abstracting with credit is permitted. To copy otherwise, to republish, to post on servers, or to redistribute to lists, requires prior specific permission and/or a fee: Request permission from Documentation, Institut français du pétrole, fax. +33 1 47 52 70 78, or [revueogst@ifp.fr](mailto:revueogst@ifp.fr).